

Article

**Ion Chemistry of 1H-1,2,3-Triazole. 2. Photoelectron  
Spectrum of the Iminodiazomethyl Anion and Collision  
Induced Dissociation of the 1,2,3-Triazolide Ion**

Takatoshi Ichino, Shuji Kato, Scott W. Wren, Veronica M. Bierbaum, and W. Carl Lineberger

*J. Phys. Chem. A*, **2008**, 112 (40), 9723-9730 • DOI: 10.1021/jp805023n • Publication Date (Web): 06 September 2008

Downloaded from <http://pubs.acs.org> on November 26, 2008

**More About This Article**

Additional resources and features associated with this article are available within the HTML version:

- Supporting Information
- Access to high resolution figures
- Links to articles and content related to this article
- Copyright permission to reproduce figures and/or text from this article

[View the Full Text HTML](#)

## Ion Chemistry of 1*H*-1,2,3-Triazole. 2. Photoelectron Spectrum of the Iminodiazomethyl Anion and Collision Induced Dissociation of the 1,2,3-Triazolide Ion

Takatoshi Ichino,<sup>†</sup> Shuji Kato, Scott W. Wren, Veronica M. Bierbaum, and W. Carl Lineberger\*

JILA, University of Colorado and National Institute of Standards and Technology, and Department of Chemistry and Biochemistry, University of Colorado, Boulder, Colorado 80309-0440

Received: June 7, 2008; Revised Manuscript Received: July 14, 2008

The 363.8 nm photoelectron spectrum of the iminodiazomethyl anion has been measured. The anion is synthesized through the reaction of the hydroxide ion (HO<sup>-</sup>) with 1*H*-1,2,3-triazole in helium buffer gas in a flowing afterglow ion source. The observed spectrum exhibits well-resolved vibronic structure of the iminodiazomethyl radical. Electronic structure calculations have been performed at the B3LYP/6-311++G(d,p) level of theory to study the molecular structure of the ion. Equilibrium geometries of four possible conformers of the iminodiazomethyl anion have been obtained from the calculations. Spectral simulations have been performed on the basis of the calculated geometries and normal modes of these conformationally isomeric ions and the corresponding radicals. The spectral analysis suggests that the ions of two conformations are primarily formed in the aforementioned reaction. The relative abundance of the two conformers substantially deviates from the thermal equilibrium populations, and it reflects the potential energy surfaces relevant to conformational isomerization processes. The electron affinities of the (*ZE*)- and (*EE*)-iminodiazomethyl radicals have been determined to be  $2.484 \pm 0.007$  and  $2.460 \pm 0.007$  eV, respectively. The energetics of the iminodiazomethyl anion is compared with that of the most stable structural isomer, the 1,2,3-triazolide ion. Collision-induced dissociation of the 1,2,3-triazolide ion has also been studied in flowing afterglow-selected ion flow tube experiments. Facile fragmentation generating a product ion of *m/z* 40 has been observed. DFT calculations suggest that fragmentation of the 1,2,3-triazolide ion to the cyanomethyl anion and N<sub>2</sub> is exothermic. The stability of the ion is discussed in comparison with other azolide ions with different numbers of N atoms in the five-membered ring.

### Introduction

We have recently reported our experimental and computational study of the ion chemistry of 1*H*-1,2,3-triazole.<sup>1</sup> We found that the reaction of the hydroxide ion (HO<sup>-</sup>) with the triazole proceeds through multiple reaction pathways. Elucidation of the reaction mechanism was presented, and it was compared with those of the corresponding ion reactions for the isoelectronic azole systems we have previously studied.<sup>2–4</sup> This comparison effectively illuminates how the N atoms in the five-membered, aromatic ring affect the ion reactivity and energetics. The present study extends this previous study of the triazole system to further explore the ion energetics.

In the aforementioned study, it was concluded that, in HO<sup>-</sup> reaction with 1*H*-1,2,3-triazole, deprotonation takes place at all sites of the triazole, leading to formation of distinct ion products.<sup>1</sup> When deprotonation takes place at the C4–H site, the triazole ring opens to yield the iminodiazomethyl anion (see Figure 1 for the molecular structure). The photoelectron spectrum of the iminodiazomethyl anion was presented in the article,<sup>1</sup> but no detailed analysis of the spectrum was given. The iminodiazomethyl anion is isoelectronic with the vinyl diazomethyl anion. Previously, we reported the photoelectron spectrum of the vinyl diazomethyl anion produced from the reaction of the allyl anion with N<sub>2</sub>O.<sup>5</sup> The spectral analysis based on electronic structure calculations employing density functional

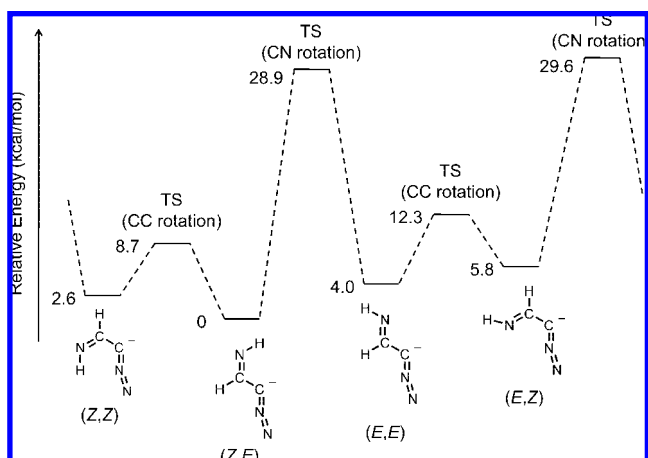


**Figure 1.** Energy diagram (electronic energy plus zero-point vibrational energy) for the conformational isomers of the iminodiazomethyl anion evaluated with B3LYP/6-311++G(d,p) calculations.

theory (DFT) offers insight into the conformational structure of the vinyl diazomethyl anion. In the present study, we have conducted further photoelectron spectroscopic measurements for the iminodiazomethyl anion and analyzed the spectrum to better understand the structure and energetics of the ion.

Formation of the iminodiazomethyl anion is not the only reaction mode that ruptures the aromatic triazole ring in the HO<sup>-</sup> reaction with 1*H*-1,2,3-triazole. Fragmentation to the ketenimine anion and N<sub>2</sub> has also been observed in the reaction.<sup>1</sup>

\* Corresponding author. E-mail: wcl@jila.colorado.edu.

<sup>†</sup> Present address: Department of Chemistry and Biochemistry, The University of Texas at Austin.

These types of processes have not been observed in the azoles containing fewer N atoms in the ring.<sup>2–4</sup> To better characterize the stability of the triazole ring, collision-induced dissociation (CID) of the 1,2,3-triazolide ion has also been examined in the present study.

### Experimental Methods

The ultraviolet negative ion photoelectron spectrometer has been described in detail in the literature.<sup>6–8</sup> A microwave discharge of helium buffer gas (~0.4 Torr) containing a small amount of O<sub>2</sub> generates the atomic oxygen radical anion (O<sup>-</sup>) in a flowing afterglow ion source. Conversion of O<sup>-</sup> to HO<sup>-</sup> ensues when O<sup>-</sup> reacts with methane introduced downstream. Subsequently, HO<sup>-</sup> reacts with 1*H*-1,2,3-triazole (Aldrich, 97%) introduced further downstream to produce the iminodiazomethyl anion. It should be noted that this reaction yields a mixture of *m/z* 68 ions, i.e., the 1,2,3-triazolide ion, 2*H*-1,2,3-triazol-4-ide ion and the iminodiazomethyl anion.<sup>1,9</sup> The ions are thermalized through collisions with helium buffer gas in a flow tube at room temperature. The flow tube is also cooled with a flow of liquid nitrogen for some measurements, so that the temperature of the ions can be lowered to ≲200 K. The anions are extracted into a differentially pumped region, accelerated to 740 eV, and focused into a Wien velocity filter for mass selection. The mass-selected ions are refocused and decelerated to 35 eV into an interaction region where the ion beam is overlapped with a laser beam in an external high-vacuum build-up cavity. The output of a continuous wave argon ion laser (363.8 nm, 3.408 eV) is amplified in the cavity with a circulating power of ~100 W. A typical beam current for *m/z* 68 ions is 300 pA.

Photodetached electrons emitted into a small solid angle perpendicular to both the ion and laser beams are focused into a hemispherical kinetic energy analyzer with a kinetic energy resolution of 8–10 meV. The energy-analyzed electrons are magnified onto the microchannel plates and imaged onto the position sensitive detector. The electron kinetic energy (eKE) settings for the analyzer are varied to construct photoelectron spectra. The electron binding energy (eBE) is the laser photon energy minus eKE. The absolute kinetic energy is calibrated in the measurements of the photoelectron spectrum of O<sup>-</sup> with respect to the very accurately known electron affinity (EA) of the O atom.<sup>10</sup> A small (<1%) compression factor<sup>8</sup> is determined to calibrate the energy scale in the measurements of the photoelectron spectra of O<sup>-</sup>, S<sup>-</sup>, and I<sup>-</sup> utilizing the EAs of the corresponding atoms.<sup>11</sup> A rotatable half-wave plate controls the angle ( $\theta$ ) between the electric field vector of the laser beam and the photoelectron momentum vector. The differential cross section for photodetachment is expressed as follows.<sup>12</sup>

$$\frac{d\sigma}{d\Omega} = \frac{\sigma_0}{4\pi}(1 + \beta P_2(\cos \theta)) \quad (1)$$

Here,  $\sigma_0$  and  $\beta$  are the total cross section and anisotropy parameter, respectively, at a particular photoelectron kinetic energy, and  $P_2(\cos \theta)$  is the second Legendre polynomial. The measurements at the magic angle, i.e.,  $\theta = 54.7^\circ$ , provide photoelectron intensities uniformly proportional to  $\sigma_0$  at all kinetic energies.

CID of the 1,2,3-triazolide ion has been studied with a tandem flowing afterglow-selected ion flow tube (FA-SIFT) instrument.<sup>13,14</sup> The experimental procedures are analogous to those reported in previous publications.<sup>1–5</sup> The 1,2,3-triazolide ion is synthesized in the source flow tube from the HO<sup>-</sup> reaction with 1*H*-1,2,3-triazole. The *m/z* 68 ions are mass-selected with a SIFT quadrupole mass filter and injected into the second flow tube

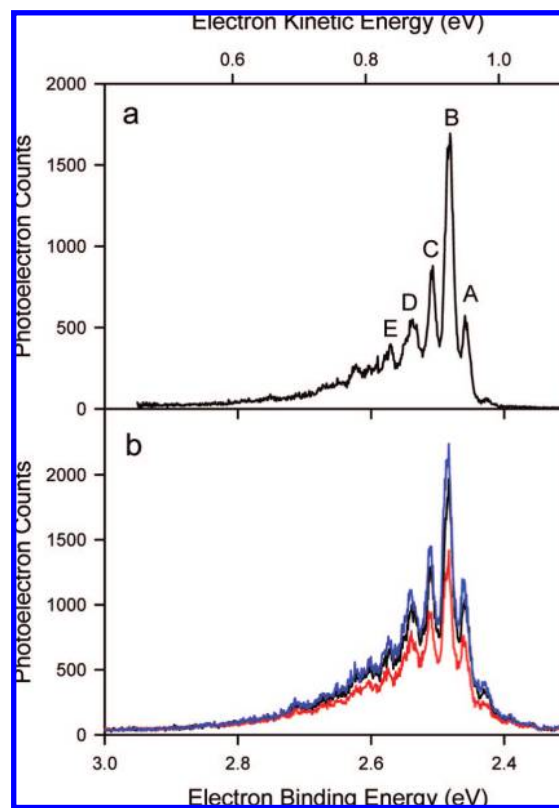


**Figure 2.** The 363.8 nm photoelectron spectra of the iminodiazomethyl anion produced from the reaction of HO<sup>-</sup> with 1*H*-1,2,3-triazole (a) in a flow tube cooled with a flow of liquid nitrogen and (b) in a flow tube at room temperature. The  $\theta$  values are 54.7° (black), 0° (red), and 90° (blue).

containing helium buffer gas (~0.5 Torr) at different injection energies (10–80 eV laboratory energy). CID takes place upon collision of the ion with the helium buffer gas in the vicinity of the injection orifice. The reactant and product ions are analyzed using a detection quadrupole mass filter at the end of the second flow tube. CID threshold energies determined in the experiments, where multiple collisions can occur during excitation and dissociation of the ion, are semiquantitatively calibrated to those corresponding to single-collision conditions, following the procedure described previously.<sup>5</sup>

### Results and Discussion

**1. Photoelectron Spectrum of the Iminodiazomethyl Anion.** Figure 2a shows the magic angle photoelectron spectrum of the iminodiazomethyl anion produced in a flow tube cooled with a flow of liquid nitrogen. A few vibronic peaks and bands are observed in the spectrum. Spectra have also been taken at different  $\theta$  values (see eq 1) for the ion produced in a flow tube at room temperature, and they are shown in Figure 2b. The  $\beta$  value for the observed peaks is  $-0.3 \pm 0.1$ , as reported previously.<sup>1</sup>

In our previous study of the photoelectron spectrum of the vinylidiazomethyl anion,<sup>5</sup> valuable information on the conformation of the ion was obtained through the spectral analysis. There are two conformers of the vinylidiazomethyl anion. DFT calculations predict that the *E* conformer is more stable than the *Z* conformer by 2.1 kcal mol<sup>-1</sup>. When the vinylidiazomethyl anions are cooled below room temperature in the flow tube, the thermal population of the *Z* conformer is expected to be negligibly small for the photoelectron spectroscopic measurements according to the calculations. Indeed, the spectral

**TABLE 1: B3LYP/6-311++G(d,p) Optimized Geometries of Iminodiazomethyl Anion and Radical of Different Conformations and the Calculated Electron Binding Energies<sup>a</sup>**

	( <i>ZE</i> )-anion	( <i>ZZ</i> )-anion	( <i>EE</i> )-anion	( <i>EZ</i> )-anion
NN	1.1639	1.1638	1.1649	1.1590
NC <sub>α</sub>	1.2696	1.2692	1.2678	1.2733
C <sub>α</sub> C <sub>β</sub>	1.4262	1.4317	1.4175	1.4199
C <sub>β</sub> N	1.3028	1.3084	1.3080	1.3129
C <sub>β</sub> H	1.1034	1.0954	1.1114	1.1023
NH	1.0253	1.0252	1.0210	1.0223
NNC <sub>α</sub>	173.20	173.44	173.05	171.78
NC <sub>α</sub> C <sub>β</sub>	120.06	121.41	119.99	122.19
C <sub>α</sub> C <sub>β</sub> N	128.64	132.02	125.75	127.99
C <sub>α</sub> C <sub>β</sub> H	116.82	113.86	115.28	112.87
C <sub>β</sub> NH	107.61	109.24	108.35	108.62
eBE (eV)	2.535	2.543	2.444	2.340
	( <i>ZE</i> )-radical	( <i>ZZ</i> )-radical	( <i>EE</i> )-radical	( <i>EZ</i> )-radical
NN	1.1478	1.1497	1.1504	1.1427
NC <sub>α</sub>	1.2840	1.2793	1.2804	1.2887
C <sub>α</sub> C <sub>β</sub>	1.4422	1.4491	1.4400	1.4436
C <sub>β</sub> N	1.2881	1.2900	1.2884	1.2909
C <sub>β</sub> H	1.0933	1.0878	1.0983	1.0919
NH	1.0251	1.0249	1.0229	1.0232
NNC <sub>α</sub>	170.49	170.60	169.94	170.05
NC <sub>α</sub> C <sub>β</sub>	120.93	122.89	120.93	119.84
C <sub>α</sub> C <sub>β</sub> N	123.37	128.71	119.24	122.36
C <sub>α</sub> C <sub>β</sub> H	119.48	114.52	118.27	114.62
C <sub>β</sub> NH	109.54	111.69	110.05	110.56

<sup>a</sup> Bond lengths are in units of angstroms, and bond angles are in units of degrees. See Figure 1 for drawings of the molecular structures. The carbon labeling is with respect to the diazo group.

simulation indicates that the ions are virtually exclusively in the *E* conformation.<sup>5</sup>

The present analysis of the photoelectron spectrum of the iminodiazomethyl anion proceeds with these findings for the vinylidiazomethyl system in mind. Electronic structure calculations for the iminodiazomethyl system have been performed at the B3LYP/6-311++G(d,p) level of theory,<sup>15–17</sup> using the Gaussian 03 program package.<sup>18</sup> Equilibrium geometries of four conformers of the iminodiazomethyl anion (see Figure 1) have been located in the calculations under *C<sub>s</sub>* symmetry. It should be noted that replacement of the vinyl group in the vinylidiazomethyl anion with an imino group results in four conformations for the iminodiazomethyl anion instead of two for the former ion.<sup>5</sup> The calculated geometrical parameters are given in Table 1. Normal mode analysis has been conducted at the equilibrium geometries and the calculated harmonic vibrational frequencies are provided in Supporting Information. All the stationary points have been found to be potential minima. Relative energies of the four conformers are shown in Figure 1. Among the conformers, the (*ZE*) conformer is the most stable energetically. The second most stable conformer is the (*ZZ*) conformer, located 2.6 kcal mol<sup>-1</sup> higher in energy than the (*ZE*) conformer. These calculations suggest that the iminodiazomethyl anion would be primarily in the (*ZE*) conformation at thermal equilibrium below room temperature.

DFT calculations have also been performed for the iminodiazomethyl radical. The data for the calculated equilibrium geometries are given in Table 1, and the harmonic vibrational frequencies are provided in the Supporting Information. All the stationary points are potential minima. The calculations predict the eBE of the (*ZE*)-iminodiazomethyl anion to be 2.535 eV. This value is fairly close to the eBE of the relatively intense peaks observed in the spectrum (Figure 2). The other imino-

diazomethyl anions of different conformations also have quite similar eBEs according to the DFT calculations (Table 1).

To positively identify the conformational structure of the iminodiazomethyl anion, the *PESCAL* program<sup>19,20</sup> has been employed to perform spectral simulations based on the equilibrium geometries and normal modes obtained from the DFT calculations. The simulated spectra for all the conformers are shown in Figure 3. An anion vibrational temperature of 200 K is assumed in these simulations. The simulated origin peak is set to peak B (see Figure 2), which gives an optimum simulation.<sup>21</sup> According to the simulations, spectral profiles for these conformers are quite distinct from each other.<sup>5</sup> As commented earlier, the DFT calculations suggest that the (*ZE*)-anion would be the most stable energetically (Figure 1). Indeed, the spectral simulation for the (*ZE*)-anion, shown in Figure 3a, is in fair agreement with the observed spectrum.

However, the quality of this simulation is not as good as that found for the vinylidiazomethyl anion.<sup>5</sup> Specifically, the relative intensity of peak A is significantly underestimated in the simulation in Figure 3a. Because the simulated origin peak is set to peak B, this simulation assumes peak A to represent photodetachment from vibrationally excited levels of the anion. The DFT calculations predict two low-frequency modes whose fundamental levels (and, to lesser extents, overtone and combination levels) could be populated significantly under the experimental conditions. One mode is associated with torsional motion around the CC bond, and the other is in-plane NC<sub>α</sub>C<sub>β</sub> bending, where the C<sub>α</sub> atom is directly bonded to the diazo group (see Supporting Information). The inadequacy of the simulation might be associated with insufficient population of these vibrational levels of the anion. A vibrational temperature of 200 K is a reasonable assumption for the ions produced in a flow tube cooled with a flow of liquid nitrogen. Simple increase of the anion temperature in the simulation does not improve the quality of the simulation. Figure 4 compares the observed spectrum with a simulation which assumes a vibrational temperature of 300 K for the (*ZE*)-anion. The higher anion temperature lends more intensity to the shoulder to the lower eBE side of peak B in the simulation, but it does not predict a distinct peak that resembles peak A as observed experimentally.

The discussion presented above strongly suggests that a simulation for one conformer alone cannot satisfactorily reproduce the spectral profile. Consequently, attempts have been made to simulate the spectrum with a mixture of conformers of the iminodiazomethyl anion. Thermochemical properties of the conformers evaluated in the DFT calculations suggest that the relative population of the (*ZZ*)-anion, which is the second most stable conformer, would be 0.2% of that of the (*ZE*)-anion in thermal equilibrium at 200 K. Therefore, any conformer other than the (*ZE*)-anion that could significantly contribute to the photoelectron spectrum would not be in thermal equilibrium with the (*ZE*)-anion.

For further discussion, it is useful to review the reaction energetics involved in the formation of the iminodiazomethyl anion. Figure 5 illustrates the energy diagram, evaluated with DFT calculations, for the reaction of HO<sup>-</sup> with 1*H*-1,2,3-triazole yielding the iminodiazomethyl anion as well as the 1,2,3-triazolide ion, which was presented in our previous publication.<sup>1</sup> Deprotonation of the triazole at the C4 position induces NN bond fission, leading to formation of complexes of the iminodiazomethyl anion. A question arises as to ensuing equilibration among the four conformers. There are two types of conversion processes. One involves CC rotation (shown in Figure 1 but omitted in Figure 5), and the other is CN rotation (shown in

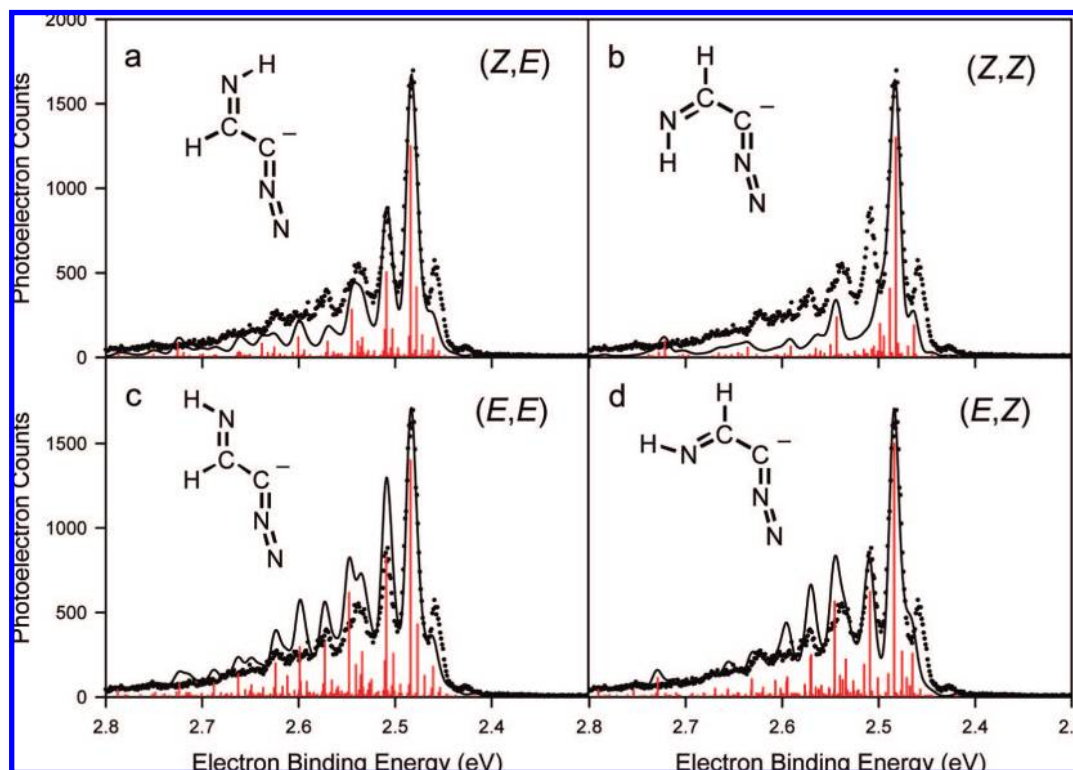


**Figure 3.** Simulations of the photoelectron spectra of the iminodiazomethyl anion of different conformations: (a) (*ZE*), (b) (*ZZ*), (c) (*EE*), and (d) (*EZ*). The sticks represent the relative positions and intensities of vibronic transitions from  $\tilde{X}^1A'$  iminodiazomethyl anion to  $\tilde{X}^2A''$  iminodiazomethyl radical. The solid lines are Gaussian convolutions of the transitions with a full width at half-maximum of 11 meV. A vibrational temperature of 200 K was assumed in the simulations. Dots are experimental data taken at the magic angle, also shown in Figure 2a.

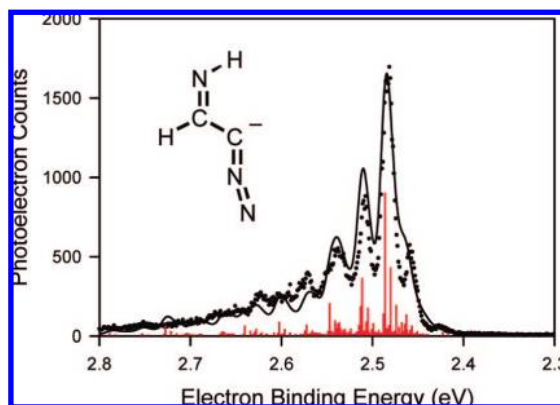


**Figure 4.** Simulation of the photoelectron spectrum of the (*ZE*)-iminodiazomethyl anion. A vibrational temperature of 300 K was assumed in the simulation. Dots are experimental data taken at the magic angle, also shown in Figure 2a.

both figures). The energy barrier for CN rotation is much higher than that for CC rotation, as shown in Figure 1. The calculated energy barrier for CN rotation in the iminodiazomethyl anion is comparable to that in iminodiazomethane.<sup>22</sup> Also, the calculated energy barrier for CC rotation in the iminodiazomethyl anion is comparable to the corresponding energy barrier in the vinylidiazomethyl anion.<sup>5</sup> While the (*ZE*)- and (*ZZ*)-anions, or the (*EE*)- and (*EZ*)-anions, would interconvert relatively easily, efficient interconversion between the (*ZE*)- and (*EE*)-anions, or between the (*ZZ*)- and (*EZ*)-anions, would be hindered by the large energy barrier. Thus, the ion–molecule complex can dissociate without a barrier to form an isolated (*EE*)-anion, whereas formation of the most stable (*ZE*)-anion can be kinetically hindered (see Figure 5). Most of the (*ZZ*)- and (*EZ*)-anions would isomerize to the (*ZE*)- and (*EE*)-anions, respec-

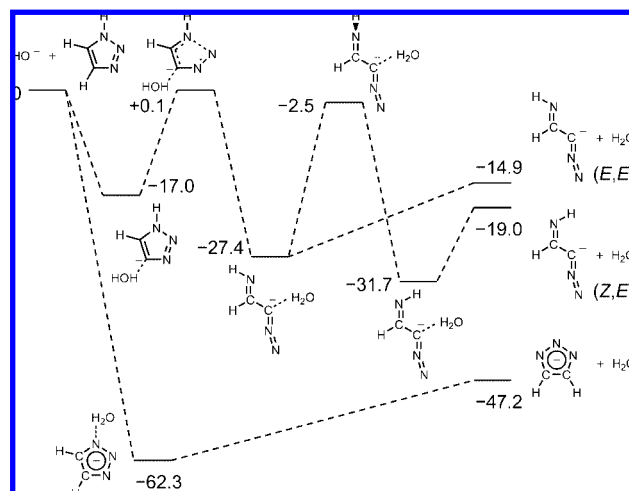


**Figure 5.** Energy diagram for the reaction of  $\text{HO}^-$  with 1*H*-1,2,3-triazole to produce the iminodiazomethyl anion and the 1,2,3-triazolide ion, evaluated with B3LYP/6-311++G(d,p) calculations. The values represent the 298 K enthalpies of the intermediate and final product states relative to that of the reactant state in units of  $\text{kcal mol}^{-1}$ .

tively, during complex dissociation. In this way, the reaction can yield the (*ZE*)- and (*EE*)-anions with nonthermal population distributions.

A simulation has been carried out under the assumption that peak A is the origin peak for photodetachment from the (*EE*)-anion whereas peak B is the origin peak for the (*ZE*)-anion. The optimum simulation is displayed in Figure 6. This simulation assumes a relative abundance of 70% (*ZE*)- and 30% (*EE*)-anions with identical photodetachment cross sections for the two conformers. Good agreement with the observed spectrum is seen when the two conformers are taken into account in the

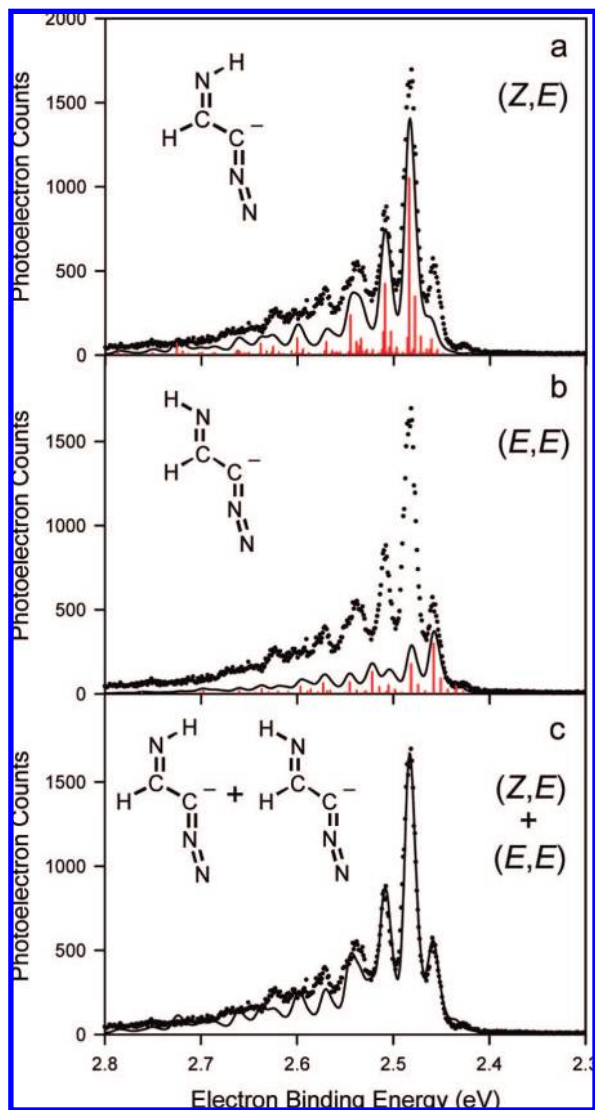


**Figure 6.** Simulations of the photoelectron spectra of (a) the (*ZE*)-iminodiazomethyl anion, (b) (*EE*)-iminodiazomethyl anion, and (c) a mixture of the (*ZE*)- and (*EE*)-anions. The simulation in (c) is the summation of those in (a) and (b). A vibrational temperature of 200 K was assumed in the simulations. Dots are experimental data taken at the magic angle, also shown in Figure 2a.

simulation (Figure 6c). On the basis of this successful simulation, it is concluded that the EAs of the (*ZE*)- and (*EE*)-iminodiazomethyl radicals are  $2.484 \pm 0.007$  and  $2.460 \pm 0.007$  eV, respectively. The DFT-calculated EA values are in good agreement with these values (see Table 1). Also, peak C represents a transition to the fundamental level of the in-plane  $\text{NC}_\alpha\text{C}_\beta$  bending mode of  $\tilde{X}^2A''$  (*ZE*)-iminodiazomethyl radical with a frequency of  $200 \pm 10$   $\text{cm}^{-1}$ . A main contribution to peak D, located  $430 \pm 25$   $\text{cm}^{-1}$  from peak B, arises from a transition to the fundamental level of the in-plane  $\text{C}_\alpha\text{C}_\beta\text{N}$  bending mode of  $\tilde{X}^2A''$  (*ZE*)-radical. Peak E, located  $735 \pm 35$   $\text{cm}^{-1}$  from peak B, largely represents a combination level of the two in-plane bending modes. It should be mentioned that the corresponding vibrational modes of the *E*-vinylidiazomethyl radical are also active in the photoelectron spectrum of the vinylidiazomethyl anion.<sup>5</sup>

Although the simulation in Figure 6c is certainly satisfactory, it is not able to exclude alternative explanations completely. For instance, a similar quality of simulation can be achieved by assuming a mixture of 90% (*ZE*)- and 10% (*ZZ*)-anions.

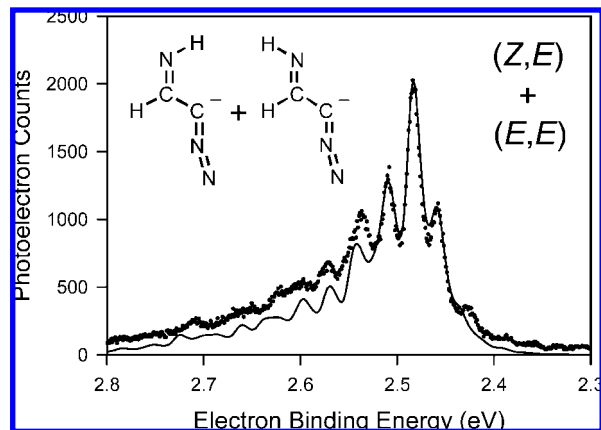
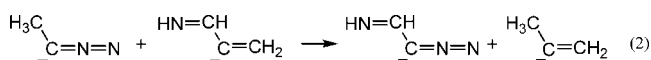


**Figure 7.** Simulation of the photoelectron spectrum of a mixture of the (*ZE*)- and (*EE*)-iminodiazomethyl anions. Gaussian convolutions were performed with a full width at half-maximum of 12 meV. A vibrational temperature of 300 K was assumed in the simulation. Dots are experimental data taken at the magic angle, also shown in Figure 2b.

Under thermal equilibrium at 200 K, this population ratio would correspond to a free energy difference of 0.9 kcal mol<sup>-1</sup> between the two conformers. The DFT calculations predict a free energy difference of 2.5 kcal mol<sup>-1</sup>. Clearly, the aforementioned conclusion favoring the mixture of the (*ZE*)- and (*EE*)-anions builds on the DFT energetics, whereas its uncertainty is not quantitatively known. However, the previous study of the vinylidiazomethyl anion<sup>5</sup> demonstrates that its photoelectron spectrum can be fully explained by making quantitative use of DFT-calculated energetics of the two conformers of the anion. For this reason, the present study supports a conclusion that a mixture of the (*ZE*)- and (*EE*)-anions account for the photoelectron spectrum of the iminodiazomethyl anion.

A similar simulation has been performed for the photoelectron spectrum of the iminodiazomethyl anion produced in a flow tube at room temperature. Figure 7 shows the result of the simulation superimposed on the observed spectrum. This simulation is based on a relative abundance of 58% (*ZE*)- and 42% (*EE*)-anions.

**2. Nitrogen Effects on the Iminodiazomethyl Systems.** The EAs of the iminodiazomethyl radicals are much larger than that of the vinylidiazomethyl radical ( $1.864 \pm 0.007$  eV).<sup>5</sup> Thus, an increase in the number of N atoms leads to an increase in the EA of the substituted diazomethyl radical. The same effect has been observed for the azolyl radicals<sup>1-4</sup> as well as for the propargyl and ketenimine radicals.<sup>1</sup> On the other hand, the magnitude of the energy stabilization of the diazomethyl anion due to the imino group is similar to that due to the vinyl group, as judged from the following isodesmic reaction,<sup>5,23,24</sup>



The stabilization energy for reaction 2 is 8.4 kcal mol<sup>-1</sup> according to B3LYP/6-311+G(d,p) calculations. The corresponding value for the vinylidiazomethyl anion<sup>5</sup> is 7.6 kcal mol<sup>-1</sup>.

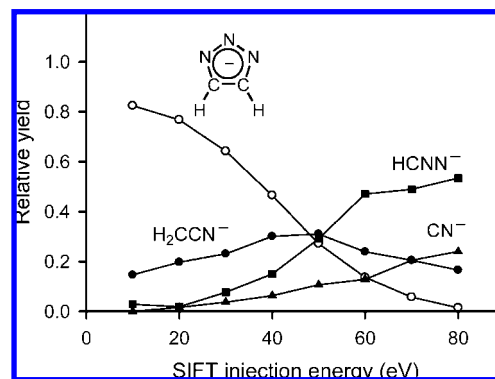
As described above, the vibronic structure of  $\tilde{X}^2A''$  iminodiazomethyl radical appears in the photoelectron spectrum in a manner similar to that of  $\tilde{X}^2A''$  vinylidiazomethyl radical. There is no clear manifestation of the electronically excited state,  $\tilde{A}^2A'$  iminodiazomethyl radical, in the photoelectron spectrum (see

Figure 2).<sup>25</sup> In contrast, the  $\tilde{A}^2A'$  state of the vinyl diazomethyl radical is observed in the photoelectron spectrum as a broad structureless band.<sup>5</sup> DFT calculations predict term energies of the  $\tilde{A}^2A'$  states of (*ZE*)- and (*EE*)-iminodiazomethyl radicals to be 0.310 and 0.229 eV, respectively. It should be mentioned that, analogous to the vinyl diazomethyl radical, the  $\tilde{X}^2A''$  and  $\tilde{A}^2A'$  states of the iminodiazomethyl radical form a quasi-Renner–Teller pair.<sup>5</sup> At the calculated equilibrium geometries of the  $\tilde{A}^2A'$  states, the  $NC_\alpha C_\beta$  angles are  $174.50^\circ$  and  $167.05^\circ$  for the (*ZE*)- and (*EE*)-radicals, respectively.<sup>26</sup> The geometry change with respect to the  $NC_\alpha C_\beta$  angle is very large in photodetachment from the iminodiazomethyl anion to the  $\tilde{A}^2A'$  state of the radical (see Table 1). DFT calculations predict vertical detachment energies of 3.305 and 3.082 eV for the  $\tilde{A}^2A'$  states of the (*ZE*)- and (*EE*)-radicals, respectively. These results of DFT calculations indicate that the laser photon energy used in the measurements is high enough to access a region of potential energy surfaces for the  $\tilde{A}^2A'$  states that could have significant Franck–Condon overlap in the photodetachment from the anion.

The absence of obvious features of the  $\tilde{A}^2A'$  state in the photoelectron spectrum is most likely due to the vibronic interaction between the  $\tilde{X}^2A''$  and  $\tilde{A}^2A'$  states of the iminodiazomethyl radical. At the equilibrium geometry of the  $\tilde{A}^2A'$  state, the potential energy of  $\tilde{X}^2A''$  (*ZE*)-iminodiazomethyl is calculated to be 0.175 eV higher than the  $\tilde{A}^2A'$  state. This energetic ordering is opposite from that for the vinyl diazomethyl radical.<sup>5</sup> The two states can nonadiabatically interact along out-of-plane normal coordinates.<sup>27</sup> Strong vibronic coupling can turn the  $\tilde{A}^2A'$  stationary point into a local maximum.<sup>28</sup> As a result, transition intensities for the photodetachment can be distributed among numerous vibronic levels, and the spectrum may appear without distinct features for the  $\tilde{A}^2A'$  state. Similar observations have been made, for instance, in the photoelectron spectrum of the pyrazolide ion.<sup>29</sup> Incidentally, this vibronic coupling may contribute to some extent to minor discrepancy between the experimental and simulated spectra in the higher eBE portion of the photoelectron spectrum (see Figure 6c).

The term energy for  $\tilde{A}^2A'$  iminodiazomethyl radical is calculated to be significantly lower than that for  $\tilde{A}^2A'$  vinyl diazomethyl radical.<sup>5</sup> The imino group substitution, which increases the number of N atoms in the system, narrows the energy gap between the  $\tilde{X}^2A''$  and  $\tilde{A}^2A'$  states. Similar effects of the N atoms have been observed for the series of the azolyl radicals.<sup>29</sup>

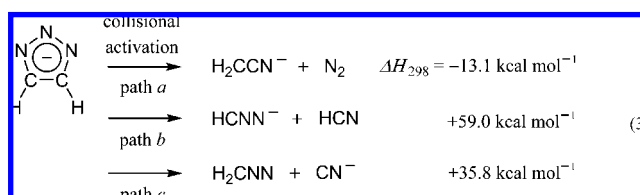
Neutral iminodiazomethanes thermally convert to the corresponding 1,2,3-triazoles via 1,5-electrocyclization.<sup>30,31</sup> Electronic structure calculations suggest that the exothermicity of the cyclization of iminodiazomethane is larger than that of the cyclization of vinyl diazomethane to the corresponding pyrazole.<sup>22</sup> The energy barrier for the cyclization has been calculated to be lower for iminodiazomethane than that for vinyl diazomethane.<sup>22,32</sup> While vinyl diazomethane requires torsion of the vinyl group out of the molecular plane for the cyclization, such distortion of the  $\pi$  molecular orbitals is not necessary for the cyclization of iminodiazomethane when it is in a favorable conformation.<sup>22</sup> In the present gas-phase negative ion study, we have observed a reverse process for the 1,2,3-triazolide ion: ring-opening through C4 deprotonation to yield the iminodiazomethyl anion. A similar process has not been observed in the  $HO^-$  reaction with pyrazole.<sup>4</sup> The more acidic property of 1*H*-1,2,3-triazole leads to its higher reactivity, as discussed previously.<sup>1</sup> There seems to be no report of base-catalyzed triazole ring-



**Figure 8.** Relative yields of the ions produced from CID of the 1,2,3-triazolide ion as a function of SIFT injection energy (laboratory frame).

opening in solution.<sup>33</sup> It has been found, however, that an analogous anion mechanism causes pyrazole ring-opening in solution.<sup>34,35</sup>

**3. CID of the 1,2,3-Triazolide Ion.** Figure 8 shows the relative yields of the product ions in CID of the 1,2,3-triazolide ion as a function of SIFT injection energy. At relatively low injection energies, the major fragmented product ions have  $m/z$  40, but as the injection energy increases, more product ions with  $m/z$  41 are observed together with a minor amount of  $m/z$  26 ions. A significant yield of  $m/z$  40 ions is observed even at the lowest injection energy (10 eV). It is assumed that the  $m/z$  40 ion is the cyanomethyl anion ( $H_2CCN^-$ , path a). B3LYP/6-311++G(d,p) calculations suggest that fragmentation of the 1,2,3-triazolide ion to  $H_2CCN^-$  and  $N_2$  is  $13.1 \text{ kcal mol}^{-1}$  exothermic.



The CID threshold energy has been estimated for the 1,2,3-triazolide ion to be roughly 1.7 eV following the calibration procedure used for other azolide ions.<sup>5</sup> This threshold energy is significantly lower than that for the pyrrolide, imidazolide and pyrazolide ions.<sup>5</sup> Unlike the triazolide ion, no exothermic fragmentation pathways have been found for these ions containing one or two N atoms in the five-membered ring in DFT calculations.<sup>5</sup> In this sense, the 1,2,3-triazolide ion is similar to a homologous ion, the pentazolide ion ( $N_5^-$ ).<sup>36,37</sup> Decomposition of  $N_5^-$  to  $N_3^-$  and  $N_2$  is predicted to be  $14 \text{ kcal mol}^{-1}$  exothermic according to CCSD(T) calculations.<sup>37</sup> Also, the energy barrier for this fragmentation has been calculated to be  $27.7 \text{ kcal mol}^{-1}$ .<sup>37</sup> On the other hand, fragmentation of the 1,2,3-triazolide ion to  $H_2CCN^-$  and  $N_2$  requires proton migration.

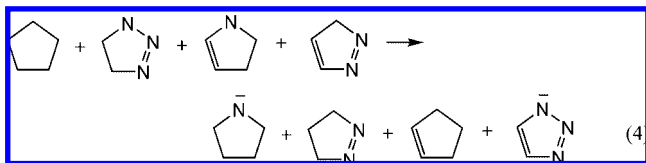
It should be cautioned that our photoelectron spectroscopic measurements reveal that the ring-opened isomer, the iminodiazomethyl anion, has also been produced in the  $HO^-$  reaction with 1*H*-1,2,3-triazole, accounting for a significant fraction of  $m/z$  68 ions (Figure 5).<sup>1</sup> DFT calculations suggest that the iminodiazomethyl anion is located  $28.3 \text{ kcal mol}^{-1}$  higher in energy than the 1,2,3-triazolide ion. Thus, this ring-opened ion may be more prone to fragmentation upon SIFT injection, and there may be small contributions from the iminodiazomethyl

anion to formation of the fragmented ions even at the lowest injection energy. If this is the case, then the threshold energy for CID of the 1,2,3-triazolide ion may be slightly underestimated.

In our previous study,<sup>1</sup> it was concluded that HO<sup>-</sup> deprotonation of 1*H*-1,2,3-triazole at the C5 position leads to fragmentation of the triazole ring, forming the ketenimine anion (HCCNH<sup>-</sup>) and N<sub>2</sub>. The identity of the ketenimine anion was confirmed in the photoelectron spectroscopic measurements.<sup>1</sup> The ketenimine anion (HCCNH<sup>-</sup>) is a structural isomer of the cyanomethyl anion (H<sub>2</sub>CCN<sup>-</sup>). In contrast to the photoelectron spectroscopic measurements, mass spectrometric detection of the CID product ions does not allow positive identification of the product ions. However, DFT calculations suggest that HCCNH<sup>-</sup> is located 28.0 kcal mol<sup>-1</sup> higher in energy than H<sub>2</sub>CCN<sup>-</sup>. Therefore, the observed low threshold energy strongly supports a conclusion that the *m/z* 40 product ion of CID of the 1,2,3-triazolide is H<sub>2</sub>CCN<sup>-</sup>.<sup>38</sup>

As for the other product ions observed in CID of the 1,2,3-triazolide, the *m/z* 41 ion is assumed to be the diazomethyl anion, and the *m/z* 26 ion is presumably the cyanide ion. Both of these fragmentation pathways are calculated to be endothermic, as shown in reaction 3. More diazomethyl anions (path b) were observed than cyanide ion (path c), even though path c is energetically more favorable. The nascent fragmentation product complex may be relatively short-lived such that proton-transfer equilibrium is not established within the dissociation complex.

The relatively unstable nature of the 1,2,3-triazolide ion found in the CID measurements uncovers the effects of the N atoms in the azolide system. To better understand the N atom effects, an aromatic stabilization energy in the 1,2,3-triazolide ion has been evaluated with a homodesmotic reaction,<sup>39–41</sup> which is analogous to one employed for the pyrazolide system.<sup>5</sup>



The aromatic stabilization energy has been estimated to be 26.9 kcal mol<sup>-1</sup> for the 1,2,3-triazolide ion in B3LYP/6-311++G(d,p) calculations. This value is very close to that for the pyrazolide ion.<sup>5</sup> Thus, there is no decrease in aromaticity as an additional N atom is substituted for a C–H unit in the pyrazolide ion. It is rather the particular molecular structure of the triazolide ion that could promote the fragmentation.

## Conclusion

The photoelectron spectrum of the iminodiazomethyl anion, produced in the reaction of HO<sup>-</sup> with 1*H*-1,2,3-triazole in helium buffer gas, has been measured to investigate its structure. The vibronic structure of the ground state of the iminodiazomethyl radical is reflected in the observed spectrum. B3LYP/6-311++G(d,p) calculations have been carried out for the ion and radical in different conformations, and spectral simulations have been performed on the basis of the equilibrium geometries and normal modes obtained in the electronic structure calculations. The simulations reveal that the majority of the iminodiazomethyl anions are in (*ZE*) and (*EE*) conformations, but the relative populations of the two conformers are far from thermal-equilibrium populations. It is concluded that thermal equilibration is prohibited by a high energy barrier for isomerization between the two conformers.

The EAs of the (*ZE*)- and (*EE*)-iminodiazomethyl radicals have been determined to be 2.484 ± 0.007 and 2.460 ± 0.007 eV, respectively.

CID measurements for the 1,2,3-triazolide ion provide results in striking contrast with those for the azolide ions with one or two N atoms in the five-membered ring. The CID threshold energy for the 1,2,3-triazolide ion is much lower than those for other azolide ions. Fragmentation of the 1,2,3-triazolide ion to the cyanomethyl anion and N<sub>2</sub> is exothermic according to DFT calculations. This characteristic of the 1,2,3-triazolide ion is similar to the pentazolide ion.

**Acknowledgment.** We thank Dr. Django Andrews for useful discussions. We are pleased to acknowledge generous support from the Air Force Office of Scientific Research and the National Science Foundation.

**Supporting Information Available:** Harmonic vibrational frequencies of the iminodiazomethyl anion and radical evaluated with B3LYP/6-311++G(d,p) calculations. This material is available free of charge via the Internet at <http://pubs.acs.org>.

## References and Notes

- (1) Ichino, T.; Andrews, D. H.; Rathbone, G. J.; Misaizu, F.; Calvi, R. M. D.; Wren, S. W.; Kato, S.; Bierbaum, V. M.; Lineberger, W. C. *J. Phys. Chem. B* **2008**, *112*, 545–557.
- (2) Gianola, A. J.; Ichino, T.; Hoenigman, R. L.; Kato, S.; Bierbaum, V. M.; Lineberger, W. C. *J. Phys. Chem. A* **2004**, *108*, 10326–10335.
- (3) Gianola, A. J.; Ichino, T.; Hoenigman, R. L.; Kato, S.; Bierbaum, V. M.; Lineberger, W. C. *J. Phys. Chem. A* **2005**, *109*, 11504–11514.
- (4) Gianola, A. J.; Ichino, T.; Kato, S.; Bierbaum, V. M.; Lineberger, W. C. *J. Phys. Chem. A* **2006**, *110*, 8457–8466.
- (5) Ichino, T.; Gianola, A. J.; Kato, S.; Bierbaum, V. M.; Lineberger, W. C. *J. Phys. Chem. A* **2007**, *111*, 8374–8383.
- (6) Leopold, D. G.; Murray, K. K.; Stevens Miller, A. E.; Lineberger, W. C. *J. Chem. Phys.* **1985**, *83*, 4849–4865.
- (7) Ervin, K. M.; Ho, J.; Lineberger, W. C. *J. Chem. Phys.* **1989**, *91*, 5974–5992.
- (8) Ervin, K. M.; Lineberger, W. C. *Photoelectron Spectroscopy of Negative Ions. In Advances in Gas Phase Ion Chemistry*; Adams, N. G., Babcock, L. M., Eds.; JAI Press: Greenwich, CT, 1992; Vol. 1, pp 121–166.
- (9) Owing to the different electron binding energies and relative yields, the photoelectron spectrum of the iminodiazomethyl anion is virtually free from contributions from the other structural isomers present in the ion beam (see ref 1).
- (10) Neumark, D. M.; Lykke, K. R.; Andersen, T.; Lineberger, W. C. *Phys. Rev. A* **1985**, *32*, 1890–1892.
- (11) Andersen, T.; Haugen, H. K.; Hotop, H. *J. Phys. Chem. Ref. Data* **1999**, *28*, 1511–1533.
- (12) Cooper, J.; Zare, R. N. *J. Chem. Phys.* **1968**, *48*, 942–943.
- (13) Van Doren, J. M.; Barlow, S. E.; DePuy, C. H.; Bierbaum, V. M. *Int. J. Mass Spectrom. Ion Processes* **1987**, *81*, 85–100.
- (14) Bierbaum, V. M. Flow Tubes. In *Theory and Ion Chemistry*; Gross, M. L., Caprioli, R., Eds.; Encyclopedia of Mass Spectrometry, Vol. 1; Elsevier, Amsterdam, 2003; pp 98–109.
- (15) Becke, A. D. *J. Chem. Phys.* **1993**, *98*, 5648–5652.
- (16) Lee, C. T.; Yang, W. T.; Parr, R. G. *Phys. Rev. B* **1988**, *37*, 785–789.
- (17) Krishnan, R.; Binkley, J. S.; Seeger, R.; Pople, J. A. *J. Chem. Phys.* **1980**, *72*, 650–654.
- (18) Frisch, M. J. et al. *Gaussian 03*, revision B.05, Gaussian, Inc.: Pittsburgh, PA, 2003.
- (19) Ervin, K. M.; Ramond, T. M.; Davico, G. E.; Schwartz, R. L.; Casey, S. M.; Lineberger, W. C. *J. Phys. Chem. A* **2001**, *105*, 10822–10831.
- (20) Ervin, K. M., *PESCAL, Fortran program*; University of Nevada, Reno: Reno, 2003.
- (21) The DFT calculations predict the harmonic vibrational frequency of the in-plane NC<sub>α</sub>C<sub>β</sub> bending mode to be 186 cm<sup>-1</sup> for the (*ZE*)-radical. In the simulation, this frequency has been adjusted slightly to 202 cm<sup>-1</sup> to improve its matching with the observed peak position. The same adjustments have been made for all the conformers.
- (22) Fabian, W. M. F.; Bakulev, V. A.; Kappe, C. O. *J. Org. Chem.* **1998**, *63*, 5801–5805.
- (23) McAllister, M. A.; Tidwell, T. T. *J. Am. Chem. Soc.* **1992**, *114*, 6553–6555.



- (24) McAllister, M. A.; Tidwell, T. T. *J. Org. Chem.* **1994**, *59*, 4506–4515.
- (25) There is no clear sign of the excited state in the photoelectron spectrum of the iminodiazomethyl anion even when a laser beam of 351.1 nm (3.531 eV) is used.
- (26) Because of the quasi-linearity of the  $\text{NNC}_\alpha\text{C}_\beta$  nuclear framework, the second specification of the conformation is not meaningful for this excited state.
- (27) Köppel, H.; Domcke, W.; Cederbaum, L. S. *Adv. Chem. Phys.* **1984**, *57*, 59–246.
- (28) The DFT calculations find an imaginary frequency of  $213i \text{ cm}^{-1}$  along the out-of-plane  $\text{NC}_\alpha\text{C}_\beta$  bending coordinate for the excited state of the (*ZE*)-radical at its equilibrium geometry.
- (29) Ichino, T.; Gianola, A. J.; Lineberger, W. C.; Stanton, J. F. *J. Chem. Phys.* **2006**, *125*, 084312.
- (30) Taylor, E. C.; Turchi, I. J. *Chem. Rev.* **1979**, *79*, 181–231.
- (31) Huisgen, R. *Angew. Chem., Int. Ed. Engl.* **1980**, *19*, 947–973.
- (32) Labbe, G.; Mathys, G. *J. Org. Chem.* **1974**, *39*, 1778–1780.
- (33) See discussions in ref 1 for examples of anion-mediated triazole ring-fragmentation in solution.
- (34) Fusco, R.; Rosnati, V.; Pagani, G. *Tetrahedron Lett.* **1966**, 1739–1744.
- (35) Fusco, R.; Rosnati, V.; Pagani, G. *Tetrahedron Lett.* **1967**, 4541–4544.
- (36) Vij, A.; Pavlovich, J. G.; Wilson, W. W.; Vij, V.; Christe, K. O. *Angew. Chem., Int. Ed.* **2002**, *41*, 3051–3054.
- (37) Nguyen, M. T.; Ha, T. K. *Chem. Phys. Lett.* **2001**, *335*, 311–320.
- (38) Fragmentation of the 1,2,3-triazolide ion to both the ketenimine anion and the cyanomethyl anion requires H migration.
- (39) Cyranski, M. K.; Krygowski, T. M.; Katritzky, A. R.; Schleyer, P. v. R. *J. Org. Chem.* **2002**, *67*, 1333–1338.
- (40) Cyranski, M. K.; Schleyer, P. v. R.; Krygowski, T. M.; Jiao, H.; Hohlneicher, G. *Tetrahedron* **2003**, *59*, 1657–1665.
- (41) Cyranski, M. K. *Chem. Rev.* **2005**, *105*, 3773–3811.

JP805023N